Cahn–Hilliard phase field based incompressible two-phase flow simulations with Isogeometric discretizations

Babak S. Hosseini[1]

[1] TU Dortmund University
Institute of Applied Mathematics, LS III
babak.hosseini@math.tu-dortmund.de

May 11, 2017

Table of Contents

Overview

Motivation for Isogeometric Analysis (IGA)

- Industrial FEM simulation workflow: Model design with CAD software $\rightarrow$ Model transformation $\rightarrow$ Analysis $\rightarrow$ Postprocessing
- Standard modeling technology in CAD: Non-uniform rational B-splines (NURBS)

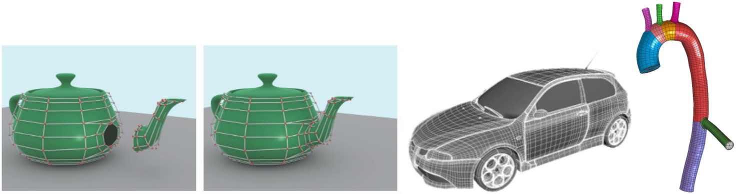

Figure: NURBS geometries taken from [9, 10, 11]

- Increasingly more complex engineering designs (Submarine: $\geq 1.000.000$ parts)
- Design to Analysis workflow: 80% modeling/20% analysis time ratio
- CAD-CAE bottleneck: Efficient creation of 'simulation-specific' geometry

Motivation for IGA

- FEM mesh only an approximation of CAD geometry

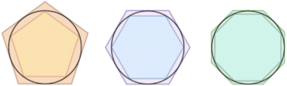

  - Shell buckling analysis very sensitive to geometric imperfections
  - Boundary layer phenomena sensitive to precise geometry configurations
  - Sliding contact between bodies cannot be accurately represented without precise geometric descriptions

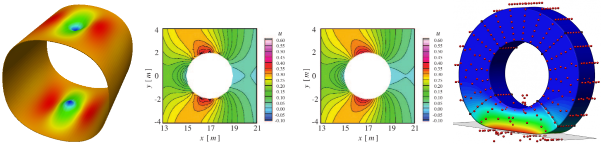

- Tighter integration of modeling-analysis process (Design optimization)
- Limited number of $\mathcal{C}^{>0}$ FE applicable to complex geometries already in 2D

Overview

Galerkin based IGA in a nutshell

- CAD and Analysis use the same geometric model (NURBS, T-splines, etc.)
- Isoparametric concept: Use the same class of functions used in CAD (B-splines, NURBS, etc.) for the PDE solution space
- Generalization of standard FEA: NURBS spaces include the piecewise polynomial spaces used in FEA
- Possibility for $\mathcal{C}^1$ and higher order continuity
- Higher-order accuracy on the degree-of-freedom basis
- Compact support
- Two- and three-dimensional geometric flexibility

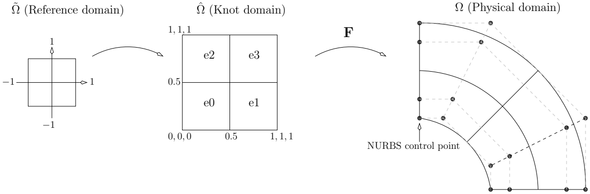

Figure: Domains involved in Isogeometric Analysis.

B-splines/NURBS in a nutshell

Define ordered knot vector $\Xi := \{\xi_1, \xi_2, \ldots, \xi_{m=n+p+1}\}$, where p is the polynomial degree, n is the number of B-spline basis functions and repetitions of knots ξ_i are allowed: $\xi_1 \leq \xi_2 \leq \cdots \leq \xi_m$.

Ξ is an open knot vector, i.e., first and last knots have multiplicities $p+1$: $\Xi = \{\underbrace{a, \ldots, a}_{p+1}, \xi_{p+2}, \ldots, \xi_{m-p-1}, \underbrace{b, \ldots, b}_{p+1}\}$.

i-th univariate B-spline function is a piecewise polynomial function, recursively defined by the Cox-de Boor recursion formula

$$B_{i,0}(\xi) = \begin{cases} 1, & \text{if } \xi_i \leq \xi < \xi_{i+1} \\ 0, & \text{otherwise} \end{cases}$$

$$B_{i,p}(\xi) = \frac{\xi - \xi_i}{\xi_{i+p} - \xi_i} B_{i,p-1}(\xi) + \frac{\xi_{i+p+1} - \xi}{\xi_{i+p+1} - \xi_{i+1}} B_{i+1,p-1}(\xi), \quad p > 0.$$

B-splines/NURBS in a nutshell

- B-spline basis functions are linearly independent and form a partition of unity: $\sum_{i=1}^{n} B_{i,p}(\xi) = 1 \quad \forall \xi \in \Xi$
- Each B-spline basis function is non-negative over entire domain: $B_{i,p}(\xi) \geq 0, \forall \xi$
- Local support property: $B_{i,p}(\xi) = 0$, if ξ outside the interval $[\xi_i, \xi_{i+p+1})$
- On each segment, we have p+1 basis functions with positive values
- At knot ξ_i the basis functions have $\alpha := p - r_i$ continuous derivatives, where r_i denotes the multiplicity of knot ξ_i

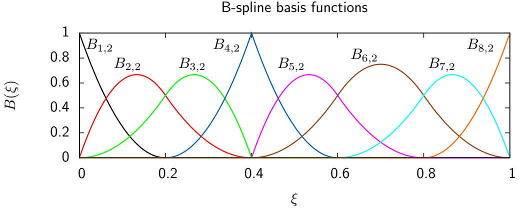

Figure: B-spline basis functions of degree $p = 2$ for open knot vector $\Xi := \{0, 0, 0, 0.2, 0.4, 0.4, 0.6, 0.8, 1, 1, 1\}$.

B-splines/NURBS in a nutshell

Derivative of i-th B-spline basis function obtained combining lower order ones:

$$\frac{d}{d\xi}B_{i,p}(\xi) = \frac{p}{\xi_{i+p} - \xi_i}B_{i,p-1}(\xi) - \frac{p}{\xi_{i+p+1} - \xi_{i+1}}B_{i+1,p-1}(\xi).$$

Augment B-splines $B_{i,p}$ with with weights w_i to obtain univariate **NURBS** basis functions (rational B-splines):

$$R_{i,p}(\xi) = \frac{B_{i,p}(\xi)w_i}{W(\xi)}, \qquad W(\xi) = \sum_{j=1}^{n} B_{j,p}(\xi)w_j.$$

First derivative of $R_{i,p}(\xi)$ is easily obtained via the quotient rule as:

$$\frac{d}{d\xi}R_{i,p}(\xi) = w_i \frac{B'_{i,p}(\xi)W(\xi) - B_{i,p}(\xi)W'(\xi)}{W^2(\xi)},$$

where $B'_{i,p}(\xi) = \frac{d}{d\xi}B_{i,p}(\xi)$ and $W'(\xi) = \sum_{i=1}^{n} B'_{i,p}(\xi)w_i$.

B-splines/NURBS in a nutshell

Space of B-splines/NURBS of degree p and regularity α determined by knot vector Ξ and spanned by the basis functions $B_{i,p}/R_{i,p}$:

$$\mathcal{S}^p_\alpha \equiv \mathcal{S}^p_\alpha(\Xi, p) := \operatorname{span}\{B_{i,p}\}_{i=1}^n$$
$$\mathcal{N}^p_\alpha \equiv \mathcal{N}^p_\alpha(\Xi, p, w) := \operatorname{span}\{R_{i,p}\}_{i=1}^n$$

Extension to higher dimensions

Consider d knot vectors Ξ_β, $1 \le \beta \le d$ and an open parametric domain $(a_d, b_d)^d \in \mathbb{R}^d$. The knot vectors Ξ_β partition the parametric domain $(a_d, b_d)^d$ into d-dimensional open knot spans, or elements, and thus yield a mesh $\mathcal{Q}$ being defined as

$$\mathcal{Q} \equiv \mathcal{Q}(\Xi_1, \ldots, \Xi_d) := \{Q = \otimes_{\beta=1}^d (\xi_{i,\beta}, \xi_{i+1,\beta}) \mid Q \neq \emptyset,\ 1 \le i < m_\beta\}$$

Tensor product B-spline and NURBS basis functions:

$$B_{i_1,\ldots,i_d} := B_{i_1,1} \otimes \cdots \otimes B_{i_d,d}, \quad i_1 = 1, \ldots, n_1, \quad i_d = 1, \ldots, n_d$$

$$R_{i_1,\ldots,i_d} := R_{i_1,1} \otimes \cdots \otimes R_{i_d,d}, \quad i_1 = 1, \ldots, n_1, \quad i_d = 1, \ldots, n_d$$

B-splines/NURBS in a nutshell

$$B_{i,j}^{p,q}(\xi,\eta) = B_{i,p}(\xi)B_{j,q}(\eta)$$

$$\frac{\partial B_{i,j}^{p,q}(\xi,\eta)}{\partial \xi} = \frac{d}{d\xi}\left(B_{i,p}(\xi)\right)B_{j,q}(\eta), \quad \frac{\partial B_{i,j}^{p,q}(\xi,\eta)}{\partial \eta} = B_{i,p}(\xi)\frac{d}{d\eta}\left(B_{j,q}(\eta)\right)$$

$$R_{i,j}^{p,q}(\xi,\eta) = \frac{B_{i,p}(\xi)B_{j,q}(\eta)w_{i,j}}{W(\xi,\eta)}$$

$$\frac{\partial R_{i,j}^{p,q}(\xi,\eta)}{\partial \xi} = w_{i,j}\frac{B'_{i,p}(\xi)B_{j,q}(\eta)W(\xi,\eta) - B_{i,p}(\xi)B_{j,q}(\eta)W'_{\xi}(\xi,\eta)}{W^2(\xi,\eta)}$$

$$\frac{\partial R_{i,j}^{p,q}(\xi,\eta)}{\partial \eta} = w_{i,j}\frac{B_{i,p}(\xi)B'_{j,q}(\eta)W(\xi,\eta) - B_{i,p}(\xi)B_{j,q}(\eta)W'_{\eta}(\xi,\eta)}{W^2(\xi,\eta)}$$

$$W'_{\xi}(\xi,\eta) = \sum_{i=1}^{n}\sum_{j=1}^{m} B'_{i,p}(\xi)B_{j,q}(\eta)w_{i,j}, \quad W'_{\eta}(\xi,\eta) = \sum_{i=1}^{n}\sum_{j=1}^{m} B_{i,p}(\xi)B'_{j,q}(\eta)w_{i,j}$$

$$W(\xi,\eta) = \sum_{i=1}^{n}\sum_{j=1}^{m} B_{i,p}(\xi)B_{j,q}(\eta)w_{i,j}$$

B-splines/NURBS in a nutshell

Tensor product B-spline and NURBS spaces

$$\mathcal{S}^{p_1,\dots,p_d}_{\alpha_1,\dots,\alpha_d} \equiv \mathcal{S}^{p_1,\dots,p_d}_{\alpha_1,\dots,\alpha_d}(\mathcal{Q}) := \mathcal{S}^{p_1}_{\alpha_1} \otimes \cdots \otimes \mathcal{S}^{p_d}_{\alpha_d} = \mathrm{span}\{B_{i_1\dots i_d}\}^{n_1,\dots,n_d}_{i_1=1,\dots,i_d=1}$$

$$\mathcal{N}^{p_1,\dots,p_d}_{\alpha_1,\dots,\alpha_d} \equiv \mathcal{N}^{p_1,\dots,p_d}_{\alpha_1,\dots,\alpha_d}(\mathcal{Q}) := \mathcal{N}^{p_1}_{\alpha_1} \otimes \cdots \otimes \mathcal{N}^{p_d}_{\alpha_d} = \mathrm{span}\{R_{i_1\dots i_d}\}^{n_1,\dots,n_d}_{i_1=1,\dots,i_d=1}$$

Spaces fully characterized by mesh $\mathcal{Q}$, degrees $p_1,\dots,p_d$ of basis functions and their continuities $\alpha_1,\dots,\alpha_d$.

Representation in the physical domain Ω

NURBS geometrical map $\mathbf{F} : \hat{\Omega} \to \Omega$

$$\mathbf{F} = \sum_{i_1=1}^{n_1} \cdots \sum_{i_d=1}^{n_d} R_{i_1}(\xi_{i_1}) \dots R_{i_d}(\xi_{i_d}) \mathbf{P}_{i_1,\dots,i_d}$$

Space $\mathcal{V}$ of NURBS basis functions on Ω, as *push-forward* of space $\mathcal{N}$

$$\mathcal{V}^{p_1,\dots,p_d}_{\alpha_1,\dots,\alpha_d} := \mathcal{V}^{p_1}_{\alpha_1} \otimes \cdots \otimes \mathcal{V}^{p_d}_{\alpha_d} = \mathrm{span}\{R_{i_1\dots i_d} \circ \mathbf{F}^{-1}\}^{n_1,\dots,n_d}_{i_1=1,\dots,i_d=1}$$

B-splines/NURBS in a nutshell

[1] **,,bent" Sobolev space** of order $m \in \mathbb{N}$

$$\mathcal{H}^m := \begin{cases} v \in L^2(\hat{\Omega}) \text{ such that} \\ v_{|Q} \in H^m(Q), \forall Q \in \mathcal{Q}, \text{ and} \\ \nabla^k(v_{|Q_1}) = \nabla^k(v_{|Q_2}) \text{ on } \partial Q_1 \cap \partial Q_2, \\ \forall k \in \mathbb{N} \text{ with } 0 \leq k \leq \min\{m_{Q_1,Q_2}, m-1\} \\ \forall Q_1, Q_2 \text{ with } \partial Q_1 \cap \partial Q_2 \neq \emptyset \end{cases}$$

with norm

$$\|v\|^2_{\mathcal{H}^m} := \sum_{i=0}^{m} |v|^2_{\mathcal{H}^i}$$

and seminorms

$$|v|^2_{\mathcal{H}^i} := \sum_{Q \in \mathcal{Q}} |v|^2_{H^i(Q)}, \; 0 \leq i \leq m$$

[1] Continuity may vary throughout the domain

Approximation with NURBS in the physical domain

Fundamental error estimate for the elliptic boundary value problem in classical FEA:

$$\left\|u-u^h\right\|_m \leq C h^\beta \|u\|_r , \quad \beta=\min(p+1-m, r-m)$$

Mesh $\mathcal{K}$ in the physical space: $\mathcal{K}=\mathbf{F}(Q) := \{\mathbf{F}(\boldsymbol{\xi}) | \boldsymbol{\xi} \in Q\}$.

Theorem ([13])

Let k and l be integer indices with $0 \leq k \leq l \leq p+1$, we have

$$\sum_{K \in \mathcal{K}_h} |v-\Pi_{\mathcal{V}_h} v|^2_{\mathcal{H}_h^k(K)} \leq C_{\mathit{shape}} \sum_{K \in \mathcal{K}_h} h_K^{2(l-k)} \sum_{i=0}^{l} \|\nabla \boldsymbol{F}\|^{2(i-l)}_{L^\infty(\boldsymbol{F}^{-1}(K))} |v|^2_{H^i(K)},$$

$\forall v \in H^l(\Omega)$

Remark [13]

The NURBS space $\mathcal{V}_h$ on the physical domain Ω delivers the optimal rate of convergence, as for the classical finite element spaces of degree p.

Approximation with NURBS in the physical domain

Example: Poisson problem on a quarter ring

$$\text{find } u : \Omega \to \mathbb{R} : \begin{cases} -\nabla \cdot (\mu \nabla u) = f & \text{in } \Omega \\ u = g & \text{on } \Gamma_D \\ \mu \nabla u \cdot \boldsymbol{n} = h & \text{on } \Gamma_N \end{cases}$$

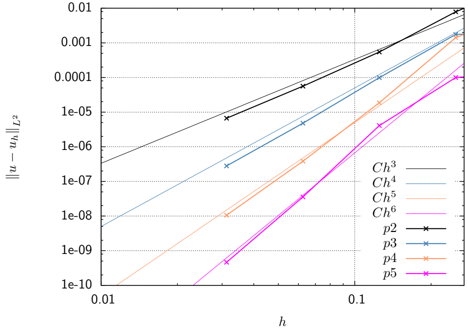

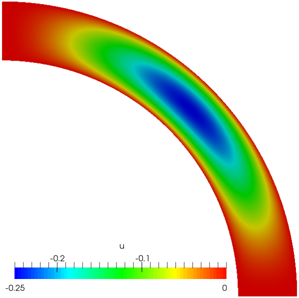

Overview

Application to two-phase flow problems

Objective: simulate **two-phase flow** problems with **large density and viscosity ratios** using the **Cahn–Hilliard phase field model**.

We would like to use a method that has the following advantages:

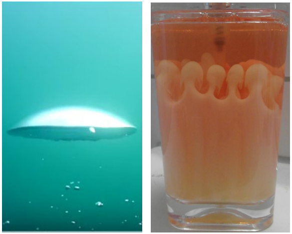

Figure: ©[7, 8]

- Complex geometries $\rightarrow$ Isogeometric Analysis
- Systematic physical approach to address interface dynamics (fluid free energy model)
- Natural handling of topological transitions
- Implicit fluid-fluid interface representation
- Modeling of interfacial forces as volume forces
- Reinitialization-free

Two-phase flow model based on fluid free energy

Classical approach:

- Force balance boundary condition

$$[\![-p\boldsymbol{I} + \mu\left(\nabla\boldsymbol{v} + (\nabla\boldsymbol{v})^T\right)]\!]\big|_\Gamma \cdot \boldsymbol{n} = \sigma\kappa\boldsymbol{n}$$

- Internal force b.c. as volumetric surface tension force

$$\boldsymbol{f}_{st} = \sigma\kappa\boldsymbol{n}\delta(\Gamma, \boldsymbol{x})$$

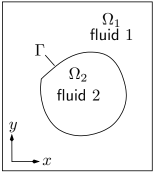

Phase field methods are based on models of fluid free energy

Simplest free energy density model for isothermal fluids yielding two phases is

$$f(\varphi) = \alpha\frac{1}{2}|\nabla\varphi|^2 + \beta\psi(\varphi) \qquad \alpha > 0, \beta > 0$$

- Order parameter $\varphi \in [-1, 1]$ measure of phase
- $\frac{1}{2}|\nabla\varphi|^2$: interfacial (surface) free energy density
- $\psi(\varphi)$: homogeneous free energy density

Principle: Energy minimization

$$\psi(\varphi) = T((1+\varphi)\log(1+\varphi) + (1-\varphi)\log(1-\varphi)) + T_c(1-\varphi^2)$$

Equilibrium interface profiles **minimize** fluid free energy (Ginzburg-Landau free energy) functional

$$\mathcal{E}(\varphi) := \int_\Omega f \,\mathrm{d}\Omega = \int_\Omega \frac{1}{2}\alpha|\nabla\varphi|^2 + \beta\psi(\varphi)\,\mathrm{d}\Omega$$

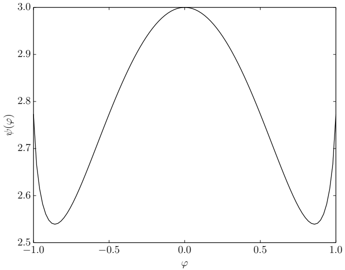

Variational derivative of $\mathcal{E}(\varphi)$ w.r.t. φ yields **chemical potential**

$$\eta = \frac{\delta\mathcal{E}}{\delta\varphi} = -\alpha\nabla^2\varphi + \beta\psi'(\varphi)$$

Equilibrium interface profiles satisfy

$$\beta\psi'(\varphi) - \alpha\nabla^2\varphi \equiv \eta = \text{const.}$$

Cahn–Hilliard system

Idea: Generalize problem to a mass diffusion equation in a binary system applying the principle of conservation of mass with a local diffusion mass flux

$$\boldsymbol{J} = -m(\varphi)\nabla\eta,$$

$$m(\varphi) = D(\varphi^2 - 1)^2$$

Mass conservation for φ requires

$$\frac{d\varphi}{dt} + \nabla \cdot \boldsymbol{J} = \frac{\partial\varphi}{\partial t} + \nabla \cdot (\boldsymbol{v}\varphi) + \nabla \cdot \boldsymbol{J} = 0$$

Advective Cahn–Hilliard (CH) equation

$$\frac{\partial\varphi}{\partial t} + \boldsymbol{v} \cdot \nabla\varphi = \nabla \cdot (m(\varphi)\nabla\eta) = \nabla \cdot \left(m(\varphi)\nabla\left(-\alpha\nabla^2\varphi + \beta\psi'(\varphi)\right)\right),$$

$$\nabla\eta \cdot \boldsymbol{n} = 0, \qquad \text{(no flux b.c.)}$$

$$\nabla\varphi \cdot \boldsymbol{n} = \frac{1}{\epsilon\sqrt{2}}\cos(\theta)(1 - \varphi^2) \qquad \text{(contact angle b.c.)}$$

State of equilibrium, surface tension

Equilibrium interface profile given by solution of equation

$$\eta(\varphi) = -\alpha\nabla^2\varphi + \beta\psi'(\varphi)^2 = -\alpha\Delta\varphi + \beta\varphi(\varphi^2 - 1) = 0$$

Solution characterized by

- two stable minima at $\varphi \approx \pm 1$ standing for the two phases
- $1D$ transition region given by

$$\varphi(x) = \tanh\left(\frac{x}{\sqrt{2}\sqrt{\alpha/\beta}}\right)$$

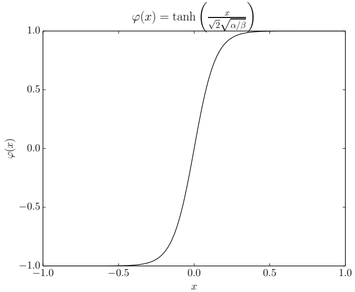

Surface tension of the interface of an isothermal fluid system in equilibrium is equal to integral of free energy density through interface:

$$\sigma = \alpha \int_{-\infty}^{\infty} \left(\frac{d\varphi}{dx}\right)^2 \mathrm{d}\boldsymbol{x} = \frac{2\sqrt{2}}{3}\sqrt{\alpha\beta}$$

[2] $\psi(\varphi) = \frac{1}{4}(\varphi - 1)^2(\varphi + 1)^2$

Mixed formulation

For general ψ:

- $\sigma \propto \sqrt{\alpha\beta}$
- $\epsilon \propto \sqrt{\alpha/\beta}$ (equilibrium interface thickness)

Introduce auxiliary interface thickness $\xi = \sqrt{\alpha/\beta}$ and set

$$\alpha = \frac{3}{2\sqrt{2}}\sigma\xi, \qquad \beta = \frac{3}{2\sqrt{2}}\frac{\sigma}{\xi}.$$

- Direct formulation of CH: 4th order spatial derivatives $\rightarrow \mathcal{C}^1$-FE
- High continuity spaces $\rightarrow$ Isogeometric Analysis
- Alternative: Mixed formulation

Mixed formulation of Advective Cahn–Hilliard equation

$$\frac{\partial\varphi}{\partial t} + \boldsymbol{v}\cdot\nabla\varphi - \nabla\cdot(m(\varphi)\nabla\eta) = 0,$$

$$\eta - \beta\,\frac{d\psi(\varphi)}{d\varphi} + \alpha\,\nabla^2\varphi = 0$$

Minimization of Ginzburg-Landau free energy

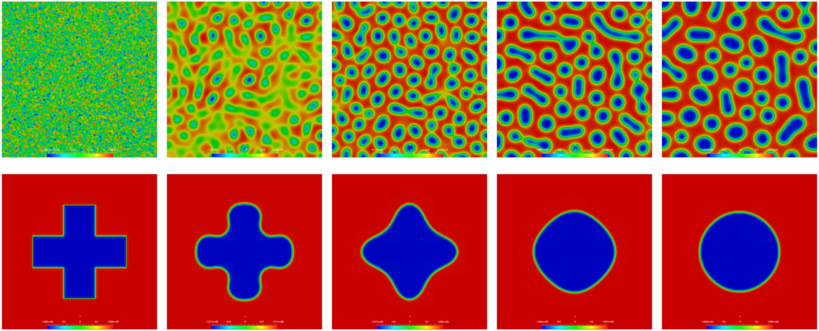

- Volume fraction of the first fluid in the mixture: $\vartheta = \frac{dV_1}{dV}$
- $\varphi = 2\vartheta - 1$
- Volume averaged density and viscosity:

$$\rho(\varphi(x,y)) = \rho_1(1+\varphi)/2 + \rho_2(1-\varphi)/2,$$
$$\mu(\varphi(x,y)) = \mu_1(1+\varphi)/2 + \mu_2(1-\varphi)/2$$

Governing equations

Navier–Stokes–Cahn–Hilliard system:

$$
\begin{aligned}
\rho(\varphi)\left(\frac{\partial \boldsymbol{v}}{\partial t} + (\boldsymbol{v}\cdot\nabla)\boldsymbol{v}\right) - \nabla\cdot\left(\mu(\varphi)\left(\nabla\boldsymbol{v} + (\nabla\boldsymbol{v})^T\right)\right) &= -\nabla p + \rho(\varphi)\boldsymbol{g} + \eta\nabla\varphi && \text{in } \Omega_T,\\
\nabla\cdot\boldsymbol{v} &= 0 && \text{in } \Omega_T,\\
\frac{\partial\varphi}{\partial t} + \boldsymbol{v}\cdot\nabla\varphi - \nabla\cdot(m(\varphi)\nabla\eta) &= 0 && \text{in } \Omega_T,\\
\eta - \beta\,\frac{d\psi(\varphi)}{d\varphi} + \alpha\,\nabla^2\varphi &= 0 && \text{in } \Omega_T,\\
\varphi(\boldsymbol{x},0) = \varphi_0(\boldsymbol{x}), \quad \boldsymbol{v}(\boldsymbol{x},0) &= \boldsymbol{v}_0(\boldsymbol{x}) && \text{in } \Omega,\\
\frac{\partial\varphi}{\partial\boldsymbol{n}} = \frac{\partial\eta}{\partial\boldsymbol{n}} = 0, \quad \boldsymbol{v} &= \boldsymbol{v}_D && \text{on } (\partial\Omega_T)_D,\\
\left(-p\boldsymbol{I} + \mu(\varphi)\left(\nabla\boldsymbol{v} + (\nabla\boldsymbol{v})^T\right)\right)\cdot\boldsymbol{n} &= \boldsymbol{t} && \text{on } (\partial\Omega_T)_N
\end{aligned}
$$

Time discretization: one-step θ-scheme (implicit)

Operator splitting solution algorithm

while $t \leq T$ **do**

1. **Solve nonlinear Advective Cahn–Hilliard system**:
   Find $(\varphi(\boldsymbol{x},t),\, \eta(\boldsymbol{x},t)) \in \mathcal{S} \times \mathcal{S} \times (0,T)$, s.t. $\forall\, q, v \in \mathcal{V}$ it holds:

   $$\mathcal{F}_{\mathsf{CH}}((\varphi,\eta);(q,v)) = 0 \qquad \text{Semilinear form}$$

   In each Newton iteration,

   $$\begin{aligned}
   &\text{Find } (\delta\varphi, \delta\eta) \in \mathcal{S} \times \mathcal{S} \times (0,T), \text{ s.t.} \\
   &\mathcal{F}'_{\mathsf{CH}}((\varphi^k,\eta^k);(\delta\varphi,\delta\eta),(q,v)) = -\mathcal{F}_{\mathsf{CH}}((\varphi^k,\eta^k);(q,v)) \qquad \forall\, q,v \in \mathcal{V} \\
   &(\varphi^{k+1},\eta^{k+1}) = (\varphi^k,\eta^k) + \omega\,(\delta\varphi,\delta\eta)
   \end{aligned}$$

2. **Solve nonlinear two-phase Navier–Stokes system**:
   Find $\boldsymbol{v}(\boldsymbol{x},t) \in \boldsymbol{\mathcal{S}} \times (0,T)$ and $p(\boldsymbol{x},t) \in \mathcal{Q} \times (0,T)$, s.t. $\forall\,(\boldsymbol{w},q) \in \boldsymbol{\mathcal{V}} \times \mathcal{Q}$ it holds

   $$\mathcal{F}_{\mathsf{NS}}(\boldsymbol{u};(\boldsymbol{w},q)) = 0 \qquad \text{Semilinear form with } \boldsymbol{u} = (\boldsymbol{v},p)$$

   In each Newton iteration,

   $$\begin{aligned}
   &\text{Find } \delta\boldsymbol{v}(\boldsymbol{x},t) \in \boldsymbol{\mathcal{S}} \times (0,T) \text{ and } \delta p(\boldsymbol{x},t) \in \mathcal{Q} \times (0,T), \text{ s.t.} \\
   &\mathcal{F}'_{\mathsf{NS}}(\boldsymbol{u}^k;\delta\boldsymbol{u},(\boldsymbol{w},q)) = -\mathcal{F}_{\mathsf{NS}}(\boldsymbol{u}^k;(\boldsymbol{w},q)) \qquad \forall\,(\boldsymbol{w},q) \in \boldsymbol{\mathcal{V}} \times \mathcal{Q} \\
   &\boldsymbol{u}^{k+1} = \boldsymbol{u}^k + \omega\,\delta\boldsymbol{u}
   \end{aligned}$$

end

Discrete Isogeometric approximation spaces

Approximation of velocity and pressure functions with LBB-stable Taylor-Hood like non-uniform rational B-spline space pairs $\hat{\mathbf{V}}_h^{TH}/\hat{Q}_h^{TH}$

$$\hat{\mathbf{V}}_h^{TH} \equiv \hat{\mathbf{V}}_h^{TH}(\mathbf{p},\boldsymbol{\alpha}) = \boldsymbol{\mathcal{N}}_{\alpha_1,\alpha_2}^{p_1+1,p_2+1} = \mathcal{N}_{\alpha_1,\alpha_2}^{p_1+1,p_2+1} \times \mathcal{N}_{\alpha_1,\alpha_2}^{p_1+1,p_2+1},$$
$$\hat{Q}_h^{TH} \equiv \hat{Q}_h^{TH}(\mathbf{p},\boldsymbol{\alpha}) = \mathcal{N}_{\alpha_1,\alpha_2}^{p_1,p_2}.$$

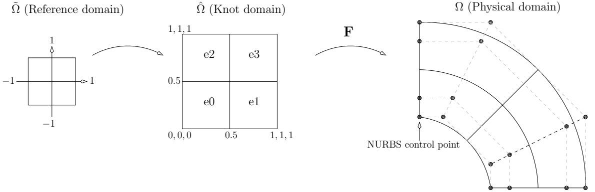

Corresponding spaces $\mathbf{V}_h^{TH}$ and Q_h^{TH} in the physical domain Ω obtained via component-wise mapping using parametrization $\mathbf{F}:\hat{\Omega}\rightarrow\Omega$

$$\mathbf{V}_h^{TH} = \{\mathbf{v} : \mathbf{v}\circ\mathbf{F} \in \hat{\mathbf{V}}_h^{TH}\} \qquad Q_h^{TH} = \{q : q\circ\mathbf{F} \in \hat{Q}_h^{TH}\}$$

Discrete problems

- Variational mixed formulation of CH problem

$$\begin{cases} \mathcal{S}^h = \mathcal{H}^1(\Omega) \cap V_h^{TH} \\ \mathcal{V}^h = \mathcal{H}_0^1(\Omega) \cap V_h^{TH} \\ \text{Find } (\varphi^h, \eta^h) \in \mathcal{S}^h \times \mathcal{S}^h \times (0,T), \text{ s.t.} \\ \mathcal{J}_{\mathsf{CH}}^h(\cdot; (\varphi^h, \eta^h), (q^h, v^h)) = \mathcal{F}_{\mathsf{CH}}(\cdot; (q^h, v^h)) \qquad \forall\, q^h, v^h \in \mathcal{V}^h \end{cases}$$

- Variational formulation of NS problem

$$\begin{cases} \boldsymbol{\mathcal{S}}^h = \boldsymbol{\mathcal{H}}^1(\Omega) \cap \mathbf{V}_h^{TH} \\ \boldsymbol{\mathcal{V}}^h = \boldsymbol{\mathcal{H}}_0^1(\Omega) \cap \mathbf{V}_h^{TH} \\ \mathcal{Q}^h = \mathcal{L}_2(\Omega)/\mathbb{R} \cap Q_h^{TH} \\ \boldsymbol{u}^h = (\boldsymbol{v}^h, p^h) \\ \text{Find } \ \boldsymbol{v}^h \in \boldsymbol{\mathcal{S}}^h \times (0,T) \ \text{ and } \ p^h \in \mathcal{Q}^h \times (0,T), \text{ s.t.} \\ \forall\, (\boldsymbol{w}^h, q^h) \in \boldsymbol{\mathcal{V}}^h \times \mathcal{Q}^h \\ \mathcal{J}_{\mathsf{NS}}(\cdot; \boldsymbol{u}^h, (\boldsymbol{w}^h, q^h)) = \mathcal{F}_{\mathsf{NS}}(\cdot; (\boldsymbol{w}^h, q^h)) \end{cases}$$

Rising bubble

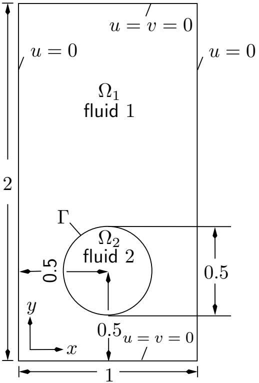

$$A_b = \int_{\Omega_2} 1 \,\mathrm{d}\boldsymbol{x},$$

$$V_b = \int_{\Omega_2} \boldsymbol{v}.y \,\mathrm{d}\boldsymbol{x}/A_b,$$

$$Y_b = \int_{\Omega_2} \boldsymbol{x}.y \,\mathrm{d}\boldsymbol{x}/A_b,$$

$$\not{c} = \frac{P_a}{P_b} = \frac{2\pi\sqrt{A_b/\pi}}{P_b},$$

$$\mathsf{EOC}_{(\cdot)} = \frac{\log(\|e_{i-1}\|_{(\cdot)}/\|e_i\|_{(\cdot)})}{\log(h_{i-1}/h_i)}$$

$$\|e\|_1 = \frac{\sum_{t=1}^{N} |q_{t,\mathsf{ref}} - q_t|}{\sum_{t=1}^{N} |q_{t,\mathsf{ref}}|},\ \|e\|_2 = \left(\frac{\sum_{t=1}^{N} |q_{t,\mathsf{ref}} - q_t|^2}{\sum_{t=1}^{N} |q_{t,\mathsf{ref}}|^2}\right)^{1/2},\ \|e\|_\infty = \frac{\max_t |q_{t,\mathsf{ref}} - q_t|}{\max_t |q_{t,\mathsf{ref}}|}$$

Test case	ρ_1	ρ_2	μ_1	μ_2	g	σ	Re	Eo	ρ_1/ρ_2	μ_1/μ_2
1	1000	100	10	1	0.98	24.5	49.5	9	10	10
2	1000	1	10	0.1	0.98	1.96	49.5	124.88	1000	100

Rising bubble, case 1, deformation over time

Phase field, IGA ($\mathcal{N}^{2,2}_{0,0} \times \mathcal{N}^{1,1}_{0,0}$)

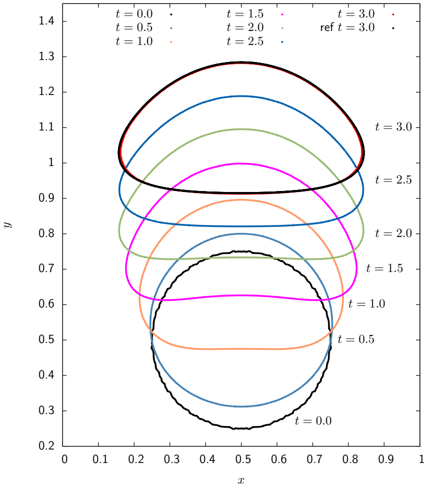

TP2D reference, Level Set, Q_2P_1 FE

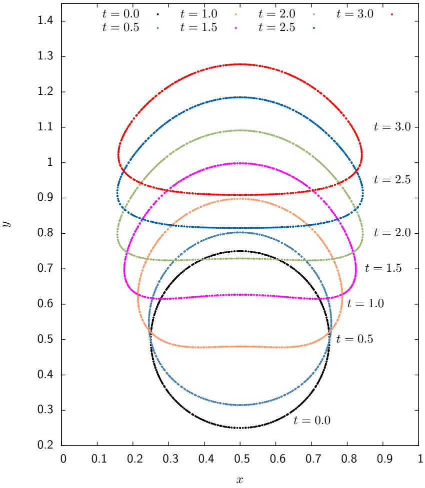

Rising bubble, case 1, quantities over time

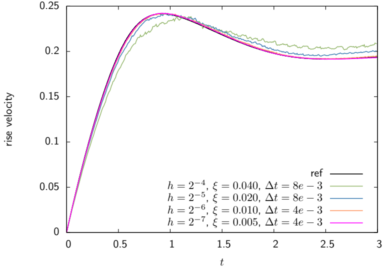

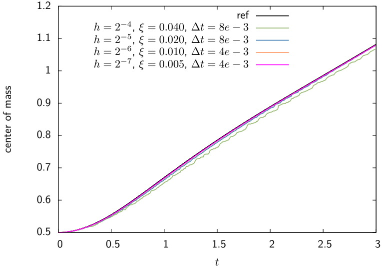

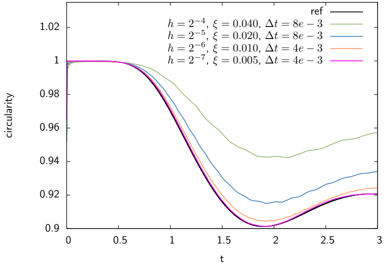

Rising bubble, case 1

h	ξ	Δt	$\not{c}_{\min}$	$t\vert_{\not{c}=\not{c}_{\min}}$	$V_{b,\max}$	$t\vert_{V_b=V_{b,\max}}$	$Y_b(t=3)$
2^{-4}	0.040	0.008	0.9425	2.1281	0.2384	1.2000	1.0665
2^{-5}	0.020	0.008	0.9151	1.9280	0.2423	0.9520	1.0778
2^{-6}	0.010	0.004	0.9044	1.9240	0.2422	0.9120	1.0792
2^{-7}	0.005	0.004	0.9013	1.9200	0.2420	0.9200	1.0794
ref			0.9013	1.9041	0.2417	0.9213	1.0813

Table: Minimum circularity and maximum rise velocity with corresponding incidence times and final center of mass position for test case 1.

Rising bubble, case 1, influence of h and ξ

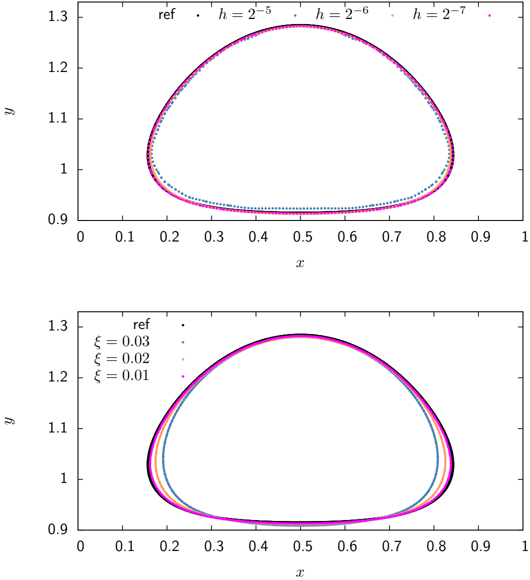

Rising bubble, case 1, convergence orders

q	h	EOC_1	$\mathrm{EOC}_1^{\mathrm{self,L7}}$	EOC_2	$\mathrm{EOC}_2^{\mathrm{self,L7}}$	EOC_∞	$\mathrm{EOC}_\infty^{\mathrm{self,L7}}$
Y_b	2^{-5}	1.7049	2.0024	1.6818	1.9263	1.4755	1.6026
	2^{-6}	1.4633	2.5718	1.5127	2.5136	1.5947	2.2132
	2^{-7}	0.5312		0.5706		0.8730	
V_b	2^{-5}	1.3263	1.3883	1.3518	1.3969	1.2714	1.2100
	2^{-6}	2.0064	2.3780	1.8934	2.3116	1.4112	2.0974
	2^{-7}	1.1755		1.0575		0.9790	
$\not{c}$	2^{-5}	1.4927	1.5363	1.5095	1.5463	1.5051	1.1128
	2^{-6}	2.0446	2.3055	2.0443	2.2597	1.9111	1.6609
	2^{-7}	2.1778		2.0334		1.6871	

- Order of convergence between 1 and ~ 2 in all norms
- Order of convergence even exceeds 2 when compared to own result

Rising bubble, case 2, deformation over time

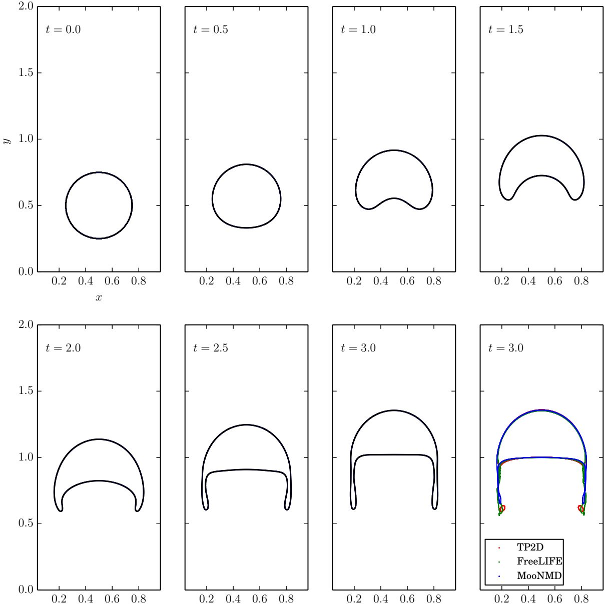

Rising bubble, case 2, final time shapes

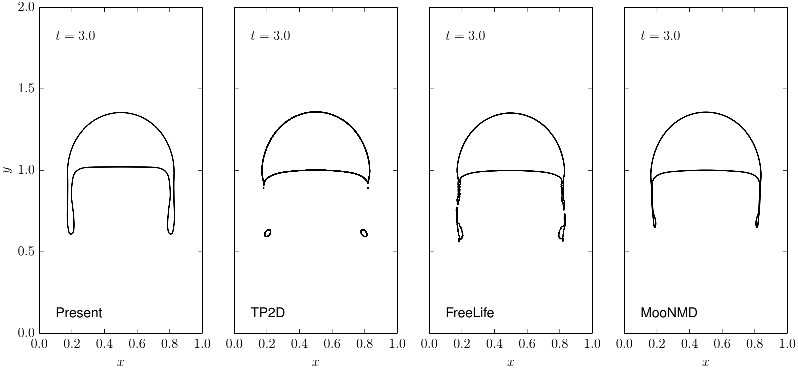

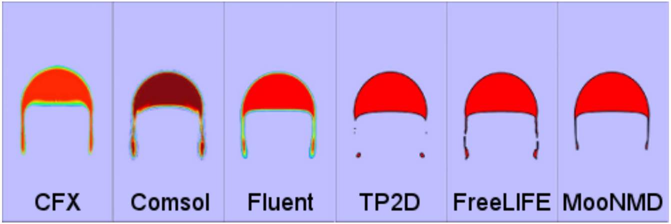

Rising bubble, case 2, quantities over time

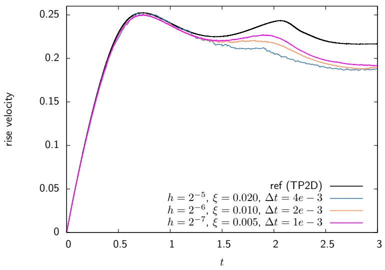

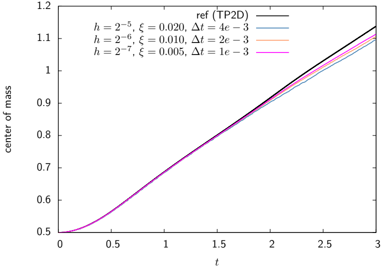

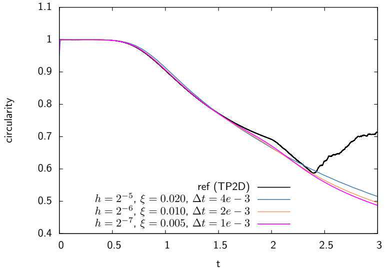

Rising bubble, case 2, convergence orders

q	h	EOC_1	$\mathsf{EOC}_1^{\mathsf{self,L7}}$	EOC_2	$\mathsf{EOC}_2^{\mathsf{self,L7}}$	EOC_∞	$\mathsf{EOC}_\infty^{\mathsf{self,L7}}$
Y_b	2^{-5}		2.0024		1.9263		1.6026
	2^{-6}	1.4620	2.5718	1.5072	2.5136	1.4755	2.2132
	2^{-7}	1.5358		1.5600		1.5947	
V_b	2^{-5}		1.3883		1.3969		1.2100
	2^{-6}	1.3060	2.3780	1.3710	2.3116	1.2714	2.0974
	2^{-7}	1.5620		1.5643		1.4112	
$\not{c}$	2^{-5}		1.5363		1.5463		1.1128
	2^{-6}	1.4147	2.3055	1.4478	2.2597	1.5051	1.6609
	2^{-7}	1.8389		1.8880		1.9111	

- Time interval confined to $[0, 2]$
- Order of convergence between 1 and ~ 2 in all norms
- Order of convergence even exceeds 2 when compared to own result

Rayleigh–Taylor instability

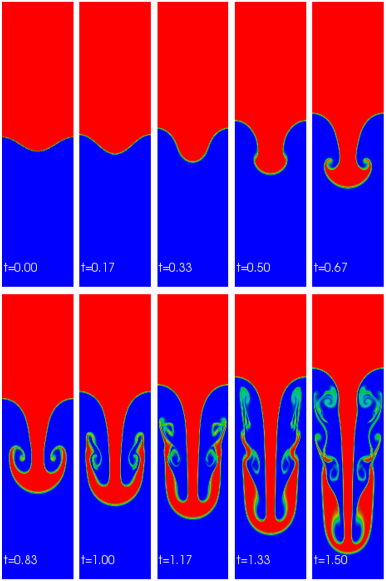

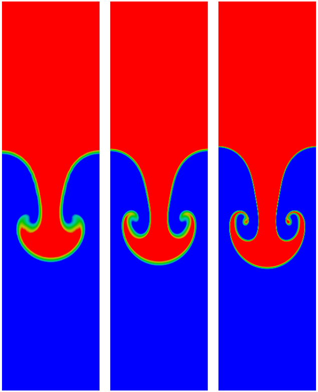

Figure: Evolution of a single wavelength initial condition for different ref. levels at $t \approx 0.8$

Rayleigh–Taylor instability

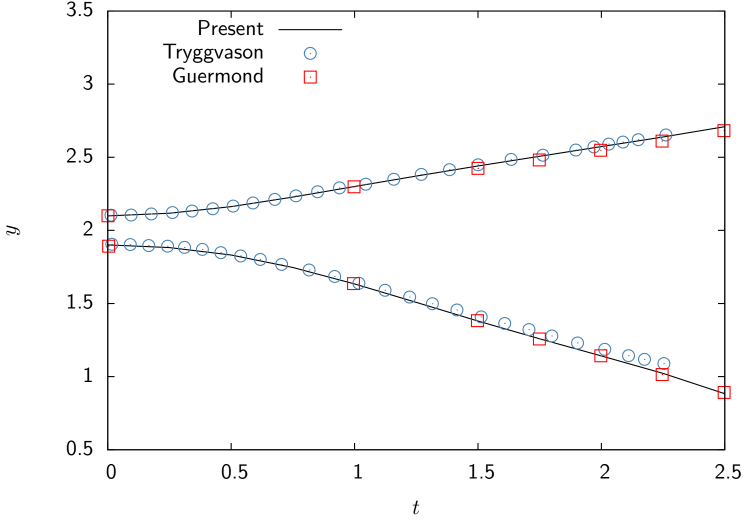

Figure: The y-coordinate of the tip of the rising and falling fluid versus time.

Conclusions and outlook

Isogeometric Analysis $\oplus$ phase field based two-phase flow model

- robust numerical method
- successful (benchmarks)

Extension to

- Complex geometries
- Multiphysics (ALE- FSI, Non-Newtonian fluids, ..)
- Local refinement (Hierarchical B-splines, T-splines, etc.)
- Multigrid
- Alternative Navier–Stokes–Cahn–Hilliard models (Abels, Boyer, ..)

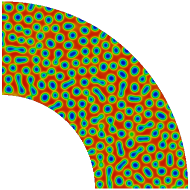

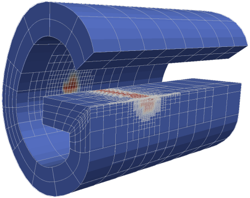

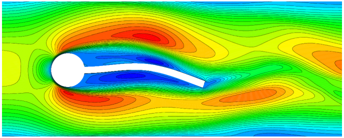

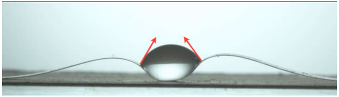

Appendix, Newton linearization (PDE level)

Linear form (for fixed φ^k, η^k):

$$
\begin{aligned}
\mathcal{F}_{\mathsf{CH}}((\varphi^k, \eta^k); \cdot) = &\int_\Omega \varphi^k\, q + \theta \Delta t \big((\boldsymbol{v} \cdot \nabla)\varphi^k\, q + m\, \nabla \eta^k \cdot \nabla q \big)\, \mathrm{d}\boldsymbol{x} \\
&- \int_\Omega \varphi^n\, q - (1-\theta)\Delta t \left((\boldsymbol{v} \cdot \nabla)\varphi^n\, q + m \nabla \eta^n \cdot \nabla q \right)\, \mathrm{d}\boldsymbol{x}, \\
&+ \int_\Omega \eta^k\, v\, \mathrm{d}\boldsymbol{x} - \int_\Omega \beta\, \psi'(\varphi^k)\, v\, \mathrm{d}\boldsymbol{x} - \int_\Omega \alpha \nabla \varphi^k \cdot \nabla v\, \mathrm{d}\boldsymbol{x}.
\end{aligned}
$$

Bilinear form $\mathcal{J}_{\mathsf{CH}} = \mathcal{F}'_{\mathsf{CH}}((\varphi^k, \eta^k); \cdot, \cdot)$ from linearization of $\mathcal{F}_{\mathsf{CH}}$ around $(\varphi, \eta) = (\varphi^k, \eta^k)$:

$$
\begin{aligned}
\mathcal{J}_{\mathsf{CH}} = &\int_\Omega \delta\varphi\, q + \theta \Delta t \left((\boldsymbol{v} \cdot \nabla)\delta\varphi\, q + m \nabla \delta\eta \cdot \nabla q \right)\, \mathrm{d}\boldsymbol{x} \\
&+ \int_\Omega \delta\eta\, v\, \mathrm{d}\boldsymbol{x} - \int_\Omega \beta\, \psi''(\varphi^k)\, \delta\varphi\, v\, \mathrm{d}\boldsymbol{x} - \int_\Omega \alpha\, \nabla \delta\varphi \cdot \nabla v\, \mathrm{d}\boldsymbol{x}
\end{aligned}
$$

Appendix, Newton linearization (PDE level)

Linear form (for fixed $\boldsymbol{u}^k$):

$$\mathcal{F}_{\mathsf{NS}}(\boldsymbol{u}^k;\cdot) = {}^3\mathcal{R}(\boldsymbol{u}^k)$$

Bilinear form $\mathcal{J}_{\mathsf{NS}} = \mathcal{F}'_{\mathsf{NS}}(\boldsymbol{u}^k; \delta\boldsymbol{u}, (\boldsymbol{w}, q))$ from linearization of $\mathcal{F}_{\mathsf{NS}}$ around $\boldsymbol{u} = \boldsymbol{u}^k$:

$$\begin{aligned}
\mathcal{J}_{\mathsf{NS}} = &\int_\Omega \rho(\varphi)\boldsymbol{w}\cdot\delta\boldsymbol{v}\,\mathrm{d}\boldsymbol{x} + \int_\Omega \mu(\varphi)\nabla\boldsymbol{w} : \left(\nabla\delta\boldsymbol{v} + (\nabla\delta\boldsymbol{v})^T\right)\,\mathrm{d}\boldsymbol{x}\\
&+ \int_\Omega \rho(\varphi)\boldsymbol{w}\cdot\delta\boldsymbol{v}\cdot\nabla\boldsymbol{v}^k\,\mathrm{d}\boldsymbol{x} + \int_\Omega \rho(\varphi)\boldsymbol{w}\cdot\boldsymbol{v}^k\cdot\nabla\delta\boldsymbol{v}\,\mathrm{d}\boldsymbol{x}\\
&- \int_\Omega \nabla\cdot\boldsymbol{w}\,\delta p\,\mathrm{d}\boldsymbol{x} + \int_\Omega q\,\nabla\cdot\delta\boldsymbol{v}\,\mathrm{d}\boldsymbol{x}
\end{aligned}$$

[3] Residual of the Navier–Stokes system

Static bubble

- $\Omega = [-1,1]^2$ with bubble centered at origin
- Finite element L^2–projection of bubble profile:

$$\int_\Omega (f - P_h f)\, w \,\mathrm{d}\boldsymbol{x} = 0, \quad \forall w \in \mathcal{W}_h$$

$$f = \varphi_{\text{bubble}}(\boldsymbol{x}) = \begin{cases} +1, & \text{for } \boldsymbol{x} \in \Omega_1 \\ -1, & \text{for } \boldsymbol{x} \in \Omega_2 \end{cases}$$

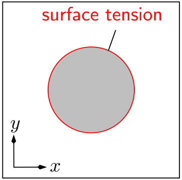

Pressure field expected to satisfy the **Laplace-Young law**

$$p_i = p_o + \sigma / r$$

$\sigma = 1, r = 1/4$

N_{el}	h	ξ	p_i	p_o	$\lvert\Delta p - (\frac{\sigma}{r})\rvert / (\frac{\sigma}{r})$	$\lvert p_i - p_o\rvert / (\frac{\sigma}{r})$	$\lVert p - p_h \rVert_{L^2}$	$\lVert \boldsymbol{v} - \boldsymbol{v_h} \rVert_{L^2}$
256	2^{-4}	0.0400	4.05234	-0.00431	0.01416	1.01416	0.539996	2.27e-04
1024	2^{-5}	0.0200	3.99563	-0.00233	0.00051	0.99949	0.379967	6.67e-05
4096	2^{-6}	0.0125	4.00642	-0.00139	0.00195	1.00195	0.296332	6.77e-05
16384	2^{-7}	0.007125	4.00067	-0.00074	0.00035	1.00035	0.222107	1.28e-04

Static bubble, pressure and spurious velocities

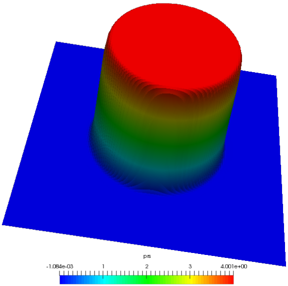

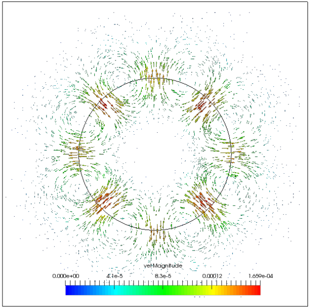

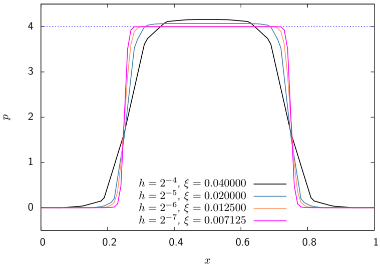

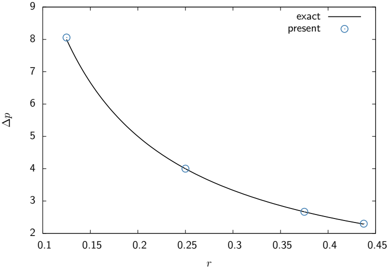

Appendix, Rising bubble, case 2, influence of h

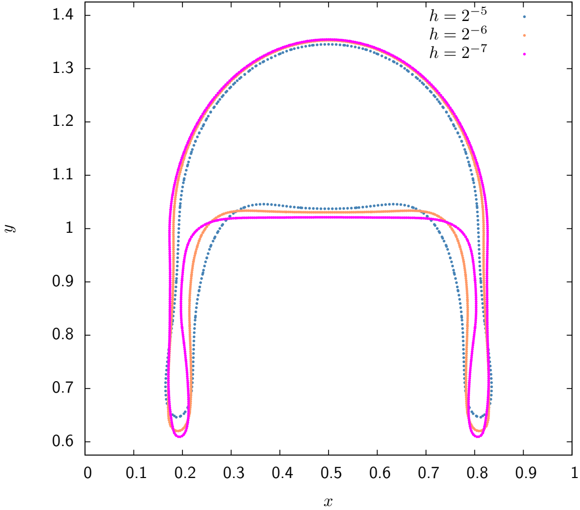

Figure: Shapes of the rising bubble at final time $t = 3$ for different h.

Appendix, Dimensionless numbers

Dimensionless numbers in the rising bubble setup:

- Reynolds number $Re = \rho_1 \tilde{v} L / \mu_1$
- Eötvös (or Bond) number $Eo = Bo = \Delta\rho g L^2 / \sigma$
- Characteristic velocity $\tilde{v} = \sqrt{g}$
- Characteristic length $L = 2r$

Appendix

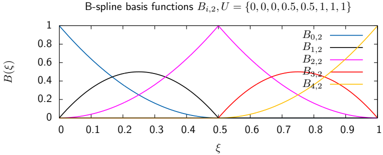

(a) $\mathcal{S}_0^2$

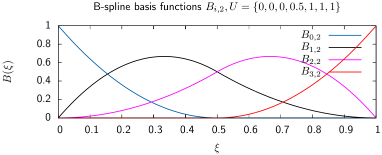

(b) $\mathcal{S}_1^2$

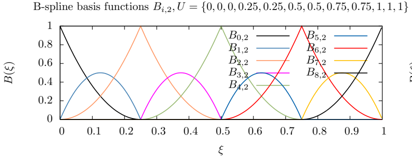

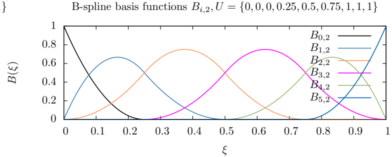

Appendix

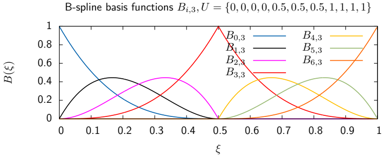

(c) $\mathcal{S}_0^3$

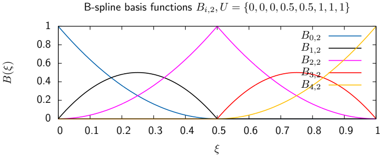

(d) $\mathcal{S}_0^2$

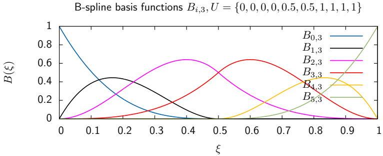

(e) $\mathcal{S}_1^3$

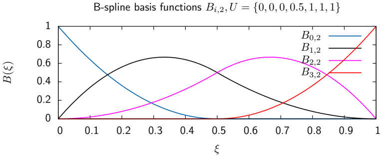

(f) $\mathcal{S}_1^2$

Appendix

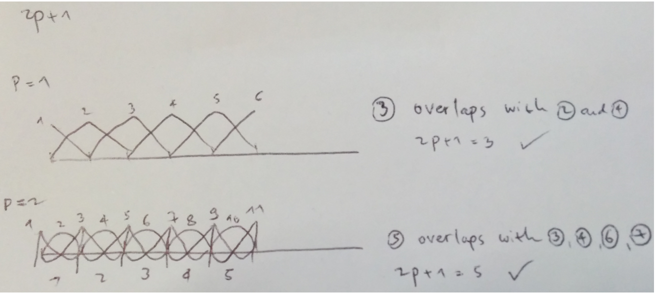

B-spline basis functions $B_{i,2}, U = \{0, 0, 0, 0.1, 0.2, 0.3, 0.4, 0.5, 0.6, 0.7, 0.8, 0.9, 1, 1, 1\}$

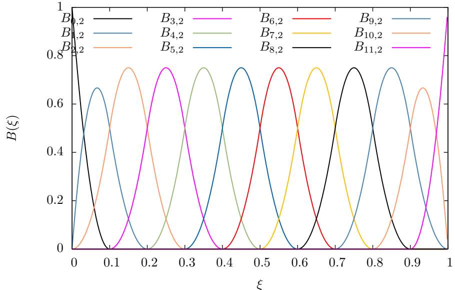

Appendix

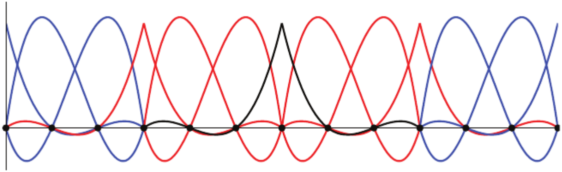

(a) Standard cubic finite element basis functions with equally spaced nodes

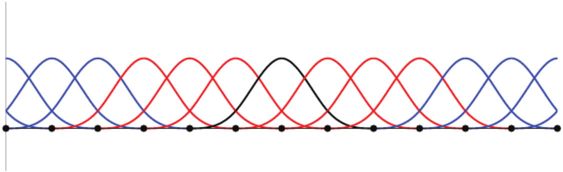

(b) Cubic B-spline basis functions with equally spaced knots

Figure: $\mathcal{C}^0$ FEA cubics vs $\mathcal{C}^2$ B-spline cubics. Bandwidth: $2p+1$ in both cases. Courtesy of Hughes et al.

Appendix, Ostwald ripening

Ostwald ripening is an observed phenomenon in solid solutions or liquid sols that describes the change of an inhomogeneous structure over time, i.e., small crystals or sol particles dissolve, and redeposit onto larger crystals or sol particles [6].

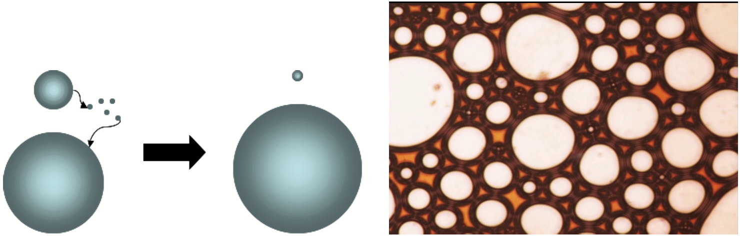

Figure: Images taken from [6]

References

Helmut Abels, Harald Garcke and Günther Grün
Thermodynamically Consistent, Frame Indifferent Diffuse Interface Models For Incompressible Two-Phase Flows With Different Densities

Hang Ding, Peter D.M. Spelt and Chang Shu
Diffuse interface model for incompressible two-phase flows with large density ratios

Babak Sayyid Hosseini, Matthias Möller and Stefan Turek
Isogeometric Analysis of the Navier-Stokes equations with Taylor-Hood B-spline elements

Babak Sayyid Hosseini, Stefan Turek, Matthias Möller and Christian Palmes
Isogeometric Analysis of the Navier–Stokes–Cahn–Hilliard equations with application to incompressible two-phase flows

FeatFlow CFD Benchmarking
http://www.featflow.de/en/benchmarks/cfdbenchmarking/bubble.html

Ostwald ripening
https://de.wikipedia.org/wiki/Ostwald-Reifung

Rayleigh Taylor instability in a soap dispenser
http://flowviz.tumblr.com/post/52065780462/an-absolutely-brilliant-example-of-the

Air Bubbles Rising in Water
https://youtu.be/NjB7LXSQoQc

T-Splines
http://www.tsplines.com

Thomas W. Sederberg et al.
Watertight Trimmed NURBS

Yongjie Zhang et al.
Patient-Specific Vascular NURBS Modeling for Isogeometric Analysis of Blood Flow.

J. Austin Cottrell, Thomas J.R. Hughes and Yuri Bazilevs
Isogeometric Analysis. Toward Integration of CAD and FEA

Y. Bazilevs, L. Beirão Da Veiga, J.A. Cottrell, T.J.R. Hughes and G. Sangalli
Isogeometric Analysis: Approximation, stability and error estimates for h-refined meshes